

# Rings in Numerical Models of Ocean General Circulation: A Statistical Study

ERIC P. CHASSIGNET

*Rosenstiel School of Marine and Atmospheric Science, University of Miami, Miami, Florida*

Because of their importance in the ocean energetics and general circulation, a proper representation of ring generation mechanisms and evolution in numerical models is crucial for an accurate picture of the heat, salt, and energy budgets. Ring locus, lifetime, propagation speed, radius, and interface displacement statistics are derived for four widely used eddy-resolving numerical models and compared to the 10-year statistical analysis of Gulf Stream rings based on time series of satellite infrared determinations performed by Brown *et al.* (1986). The ring formation process and behavior in ocean numerical models depends upon the governing equations, the vertical coordinate, and the boundary conditions used. It is shown that as more terms are retained in the model equations, the mid-latitude jet becomes more unstable, and its interior penetration as well as the associated number of rings formed are reduced. Rings in the layer model have slower propagation speeds and longer lifetimes than their level counterparts. Such results illustrate the sensitivity of numerical ocean circulation models to the physical and numerical assumptions made.

## 1. INTRODUCTION

At the present time, increasing activity in the study of the Earth's climate demands validated ocean circulation numerical models. Every model being a compromise, the all-important considerations are physical relevance, ability to interpret the results, and numerical efficiency. One therefore needs to carefully explore and explain the limitations and implications of each model choice. A systematic comparison of several eddy-resolving numerical models [Holland, 1978; Bleck and Boudra, 1986; McWilliams *et al.*, 1990; Haidvogel *et al.*, 1991] widely used by the oceanographic community for the study of oceanic processes is part of this effort.

Mid-latitude jets (Gulf Stream, Kuroshio, etc.) and associated rings play a fundamental role in the oceanic general circulation. Rings, i.e. oceanic eddies with a scale of a few hundred kilometers which detach from intense western boundary currents, represent one of the most energetic components of the world ocean mesoscale eddy field [Olson, 1991]. By virtue of their formation process, they represent an efficient mechanism by which heat, salt and potential vorticity are transferred across frontal zones, which otherwise act as barriers to mixing between different water masses. The strong nonlinear nature of these features reduces the tendency to disperse their pressure field and therefore their energy. Such coherent structures arise in oceanic numerical models when there is adequate resolution, typically of the order of 20 km, and small enough friction [Holland and Lin, 1975; Holland, 1978], and they contribute to a final statistical state in which the eddy-driven field becomes a significant part of the large-scale mean flow. The eddy and mean fields reach a mutual equilibrium with important momentum, energy, and vorticity exchange. The eddy field is also active in transferring energy downward to the deep ocean where the induced flow contributes significantly to the total mean transport. The ring formation process is interpreted in terms of barotropic and baroclinic instabilities in boundary

currents and free jets [Hurlburt and Thompson, 1980; Ikeda, 1981; Chassignet and Boudra, 1988; Spall and Robinson, 1990].

In comparisons of several adiabatic wind-driven, eddy-resolving numerical models of idealized mid-latitude basins, the ring formation process and behavior vary quite widely depending upon the governing equations, the vertical coordinate and the boundary conditions used. As more terms are retained in the model equations, the mid-latitude jet becomes more unstable and its interior penetration as well as the number of rings formed are reduced. Furthermore, rings in the layer model have slower propagation speeds and longer lifetimes than their level counterparts. Because of the importance of rings in the heat, salt, and energy budgets of the ocean, there is a need for an understanding of their generation and evolution in order to be able to reproduce accurately the general oceanic circulation in numerical models.

The layout of the paper is the following. In section 2, the model's characteristics and parameters are first reviewed and then their mean responses are described and compared. Section 3 investigates the ring formation process and evolution for the different numerical models. The ring statistics are presented in section 4. The results are then discussed in relation to observations in section 5 and as a function of the different physics and numerical implementations in section 6. The concluding section presents a summary and comments.

## 2. THE NUMERICAL MODELS

This section presents material already introduced by Chassignet and Gent [1991], but repeated here for convenience of the reader.

### 2.1. Description and Parameters

Several approximations to the Boussinesq, hydrostatic primitive equations are presently used in the oceanographic community. The popular quasi-geostrophic equations describe the flow evolution for small Rossby numbers. Specifically, the dynamical approximations that are made are the neglect of divergent velocity advection of momentum and vorticity, the neglect of variations in the Coriolis frequency, and the neglect of divergent velocity advection of buoyancy (see Pedlosky [1979] for a review). The linear balance equa-

Copyright 1992 by the American Geophysical Union.

Paper number 92JC00913.  
0148-0227/92/92JC-00913\$05.00

tions [Lorenz, 1960] are an improvement over quasi-geostrophy by relaxing the  $\beta$  plane form of the Coriolis force and the linearization of the buoyancy equation about a steady, horizontally uniform density stratification. McWilliams *et al.* [1990] showed that the essential differences observed between the quasi-geostrophic and linear balance equations are due to a more accurate treatment of the Coriolis acceleration in the latter. The linear balance equations are a subset of the balance equations [Gent and McWilliams, 1983], themselves an approximation to the primitive equations. Several primitive equation solutions have been obtained for the adiabatic case [Holland and Lin, 1975; Bleck and Boudra, 1981, 1986; Haidvogel *et al.*, 1991] as well as the diabatic case [Bryan, 1969; Cox, 1984; Semtner and Chervin, 1988; Bryan and Holland, 1989].

The equations of the four numerical models that are considered in this comparison are quasi-geostrophic (QG) [Holland, 1978; McWilliams *et al.*, 1990], linear balance (LBE) [McWilliams *et al.*, 1990], primitive with isopycnal coordinates (BB) [Bleck and Boudra, 1986] or sigma coordinates (SPEM, i.e., semi-spectral primitive equation model) [Haidvogel *et al.*, 1991]. They are all configured in a rectangular oceanic basin ( $3600 \times 2800 \times 5$  km) driven by a zonal symmetric wind forcing  $\vec{\tau} = [-\tau_m \cos(2\pi y/L), 0]$ , where  $\tau_m = 1 \times 10^{-4} \text{ m}^2 \text{ s}^{-2}$ , and damped by both a lateral eddy viscosity of the biharmonic form  $A_4 = 8 \times 10^{10} \text{ m}^4 \text{ s}^{-1}$  and a linear bottom drag ( $\nu = 2.65 \times 10^{-7} \text{ s}^{-1}$ ). The lateral boundary conditions employed on the four sidewalls are free-slip. In both horizontal coordinates, the grid is uniform with a spacing of 20 km. In the vertical, the spacing (four levels or

layers) is non uniform, with greater resolution near the upper surface. The resulting circulation is nearly anti symmetric about mid-latitude with a counterclockwise gyre north of the wind stress curl zero and clockwise south.

QG and LBE are  $z$  coordinates in the vertical with the variables located on two staggered sets of vertical grid points ( $[0, -440, -1048, -2016, -5000]$  and  $[-208, -712, -1456, -2896]$ , respectively (in meters)), defined as levels (velocity potential and buoyancy on one set and stream function on the other) [McWilliams *et al.*, 1990]. A semi spectral method [Haidvogel *et al.*, 1991] has been implemented in SPEM to solve the vertical structure ( $[0, -216, -1030, -2761, -5000]$  for the collocation points (in meters)), versus the centered, second-order finite difference scheme of QG and LBE [McWilliams *et al.*, 1990]. The BB model is a stack of shallow fluid layers ( $[440, 608, 978, 2974]$  for the mean layer thicknesses (in meters)), each one characterized by a constant value of density. The motion within each layer is governed by a momentum and a continuity equation. The layers interact through hydrostatically transmitted pressure forces. Vorticity and horizontal velocities are defined as mean layer properties. Pressure and geopotential are defined at the interfaces between layers. In all the numerical models, the initial stratification was chosen to correspond to a first baroclinic deformation radius of 44.7 km and is defined as

$$N^2(z) = -\frac{g}{\rho_0} \frac{\partial \rho}{\partial z} = 5.9 \times 10^{-5} \exp(z/800) \quad (1)$$

where  $N^2$  is in reciprocal seconds squared and  $z$  in meters.

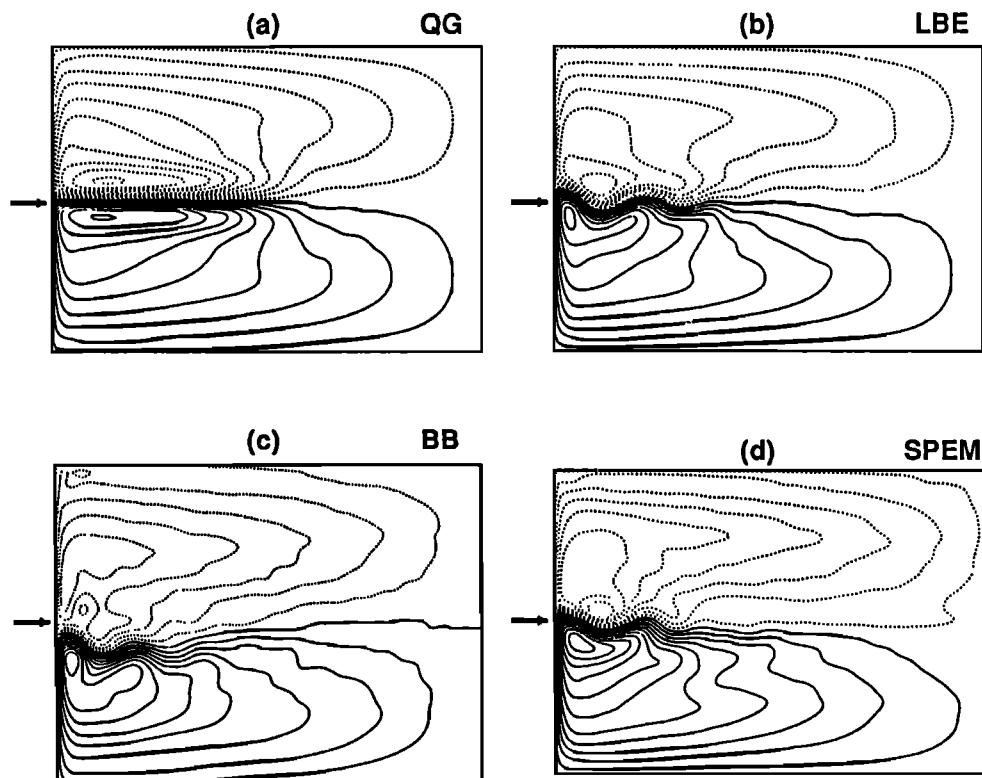


Fig. 1. Time average of the upper nondivergent stream function for the following numerical models: (a) quasi-geostrophic (QG) (40-year average), (b) linear balance (LBE) (40-year average), (c) primitive equation isopycnal coordinates (BB) (10-year average), and (d) primitive equation sigma coordinates (SPEM) (7-year average). The contour intervals are  $10^4 \text{ m}^2 \text{ s}^{-1}$  and the contour values straddle zero symmetrically. The arrow points to the zero wind stress curl line (ZWC).

For more details on the implementation of each numerical model, the reader is referred to *Bleck and Boudra* [1986], *McWilliams et al.* [1990] and, *Haidvogel et al.* [1991].

## 2.2. Mean Flow Pattern

The time average of the upper stream function for the four numerical models (obtained after a 10-year spin-up at which point statistical equilibrium was reached) are presented in Figure 1. QG differs from its counterparts by its symmetric mean response. One has to keep in mind that the approximations made to obtain the quasigeostrophic equations (see section 2.1) implies a symmetric response when a symmetric forcing is specified. As soon as the latter is relaxed, the mid-latitude jet exhibits asymmetries [*Verron and Le Provost*, 1992]. The mean path of the mid-latitude jet in the other models exhibits a standing wave pattern whose amplitude decays into the interior. The mid-latitude jet is also characterized by a reduced strength and a reduced penetration into the interior. Both LBE and SPEM show a northward penetration of the western boundary current before separation. In BB, on the contrary, the mean position of the separation point is located south of the zero wind stress curl line (ZWCL). This early separation, first noted by *Bleck and Boudra* [1981, 1986], is caused by two aspects of the numerical implementation. First, the depth over which the wind forcing acts varies in space and time in layer models but

not in level models, and this assumption was shown to have an influence upon the point of separation. Second, if the free-slip boundary is imposed as a zero vorticity condition, then an inconsistency between models arises because vorticity is not the same quantity when the governing equations are formulated in physical (level model) and isopycnal (layer model) coordinates. For more details on the mechanisms at work, the reader is referred to *Chassignet and Gent* [1991].

## 3. RING FORMATION AND EVOLUTION

Figures 2, 3, 4, and 5 display a representative set of instantaneous pictures of the upper circulation which were chosen to illustrate typical ring formation events in each of the numerical models. Characteristics of these events are summarized in Figure 6 which presents, for the four numerical models, (1) the ring location time series derived from the simulations and (2) the number of rings formed during a 10-year period in each of the three areas depicted. A ring is defined as a closed contour of a few hundred kilometers which detaches from the mid-latitude jet.

The QG mid-latitude jet (Figure 2) does not exhibit any sizeable meanders and penetrates far into the interior. Rings are observed to detach from small meanders occurring at the

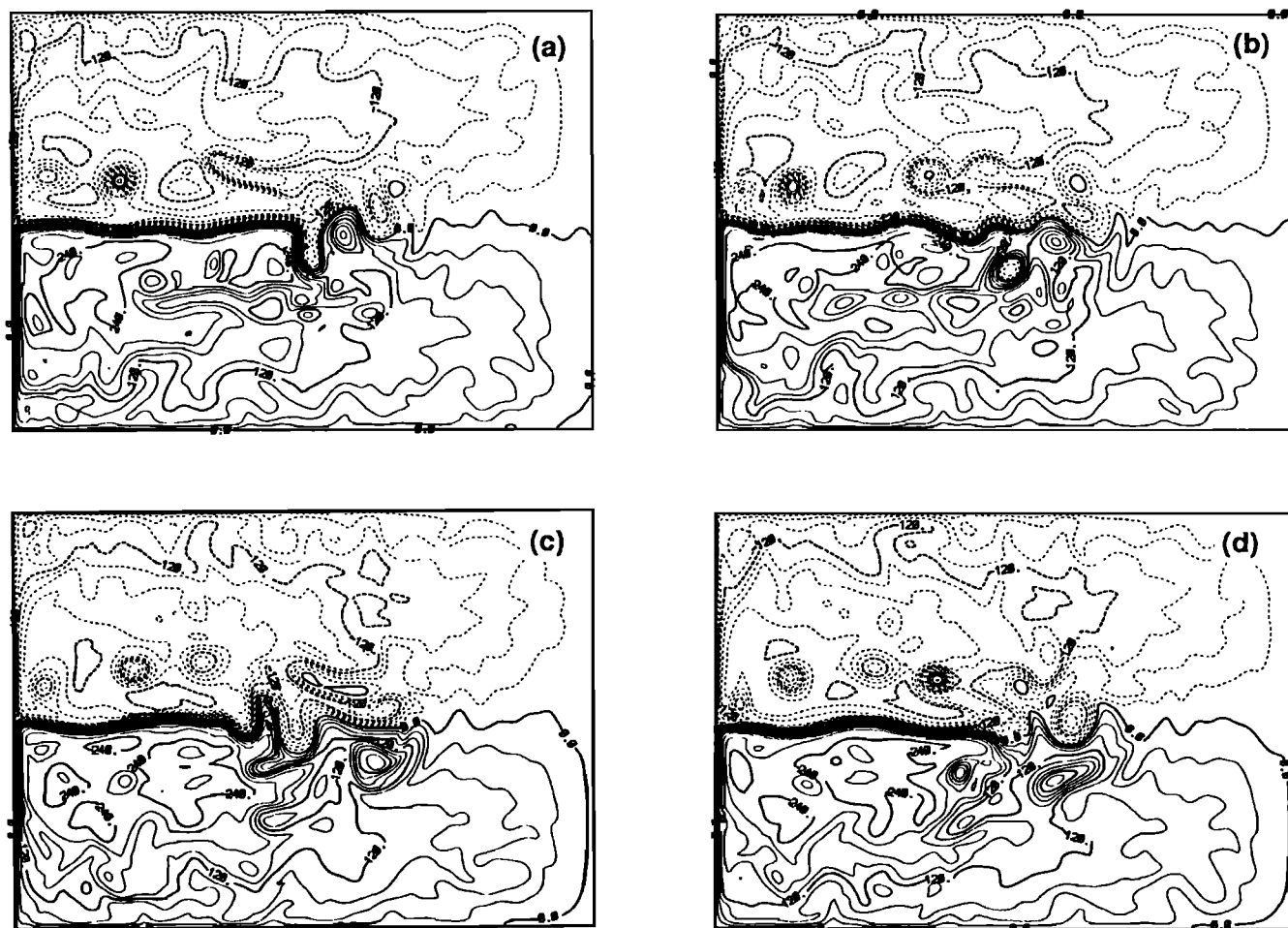


Fig. 2. Typical ring formation event for QG. Each frame represents the interface displacement anomaly in meters (contour interval (C.I.) = 30 m), and the time increment is 15 days.

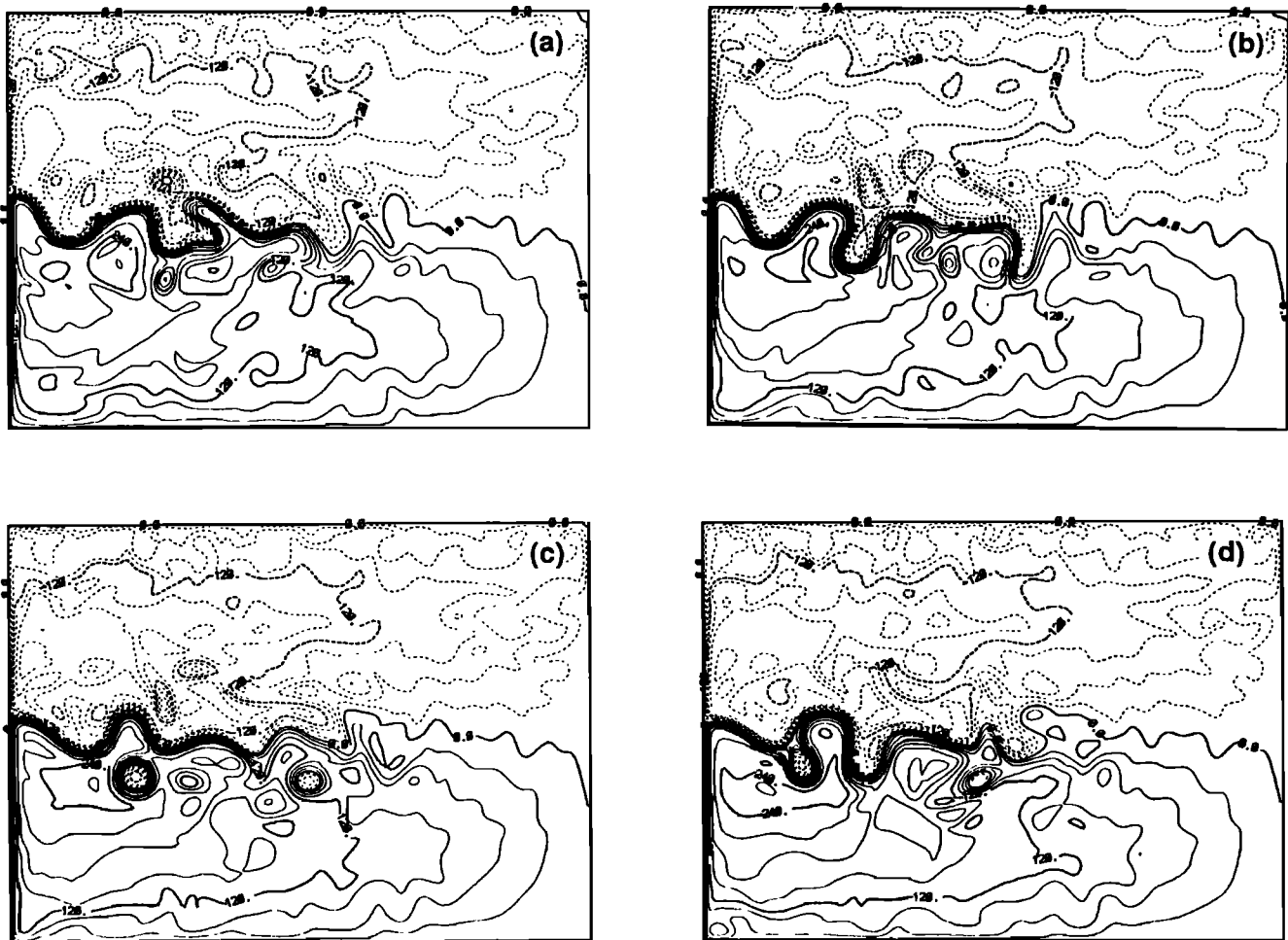


Fig. 3. Typical ring formation event for LBE. Each frame represents the interface displacement anomaly in meters (C.I. = 30 m), and the time increment is 15 days.

end of the jet. In order to quantify the ring formation process, the domain is divided into three areas (Figure 6a). Approximately 50% of the rings form in the eastern half of the domain, while the remaining 50% form in the second quarter. The ring distribution (Figure 6a) is fairly even north and south of the ZWCL. Once created, the rings propagate westward until they reach the western boundary. Occasionally, one will coalesce with the mid-latitude jet. The absence of any strong meander in the middle of the jet results from the symmetric response of the quasi-geostrophic equations to a symmetric wind forcing. In an asymmetric situation, ring generation may then occur all along the jet because of meander pinching. This was shown by Verron and Le Provost [1992] for an asymmetric wind forcing. The jet then exhibited a strong meandering structure with rings forming closer to the western boundary.

In comparison to QG, the LBE solution shows a broader, weaker jet with a shorter penetration in the interior, but with sizeable meanders as shown in Figure 3. Consequently, rings are able to form closer to the western wall than in QG through meander cutoff. In fact, almost no rings form in the eastern half of the domain, and most form in the first and second quarters (Figure 6b). Because of the strong meandering, the rings, once formed, have also more opportunities to encounter the jet and to get reabsorbed, thus a shorter

lifetime. Fewer rings than in QG actually reach the western wall, and the LBE point location cloud (Figure 6b) is then less dense than that for QG. Despite a northern separation of the jet, the LBE mid-latitude jet is on the average located south of the ZWCL (Figure 1b); the anticyclonic rings then favor a formation and propagation close to the ZWCL, while the cyclonic rings form significantly south of it.

BB's mid-latitude jet (Figure 4) penetrates slightly less into the interior than either LBE or SPEM. Most of the rings form from vigorous meanders close to the western wall, resulting in the formation of 60 to 70% of the rings in the first quarter of the domain, with the remaining ones forming in the second quarter (Figure 6c). The distribution (Figure 6c) is shifted to the south as in LBE and is consistent with both the southern separation and mean position of the mid-latitude jet (Figure 1c). Once formed, the anticyclones are observed to interact less with the jet than the cyclones and reach the western wall more easily. Actually, the most noticeable feature of Figure 6c is the presence of a high-density patch of ring loci near the western boundary of the domain which represents anticyclones decaying slowly after reaching the western wall. Interactions with the jet are not favored for these anticyclones because of the tilt in the main axis of the mid-latitude jet due to its southerly separation (Figure 1c).

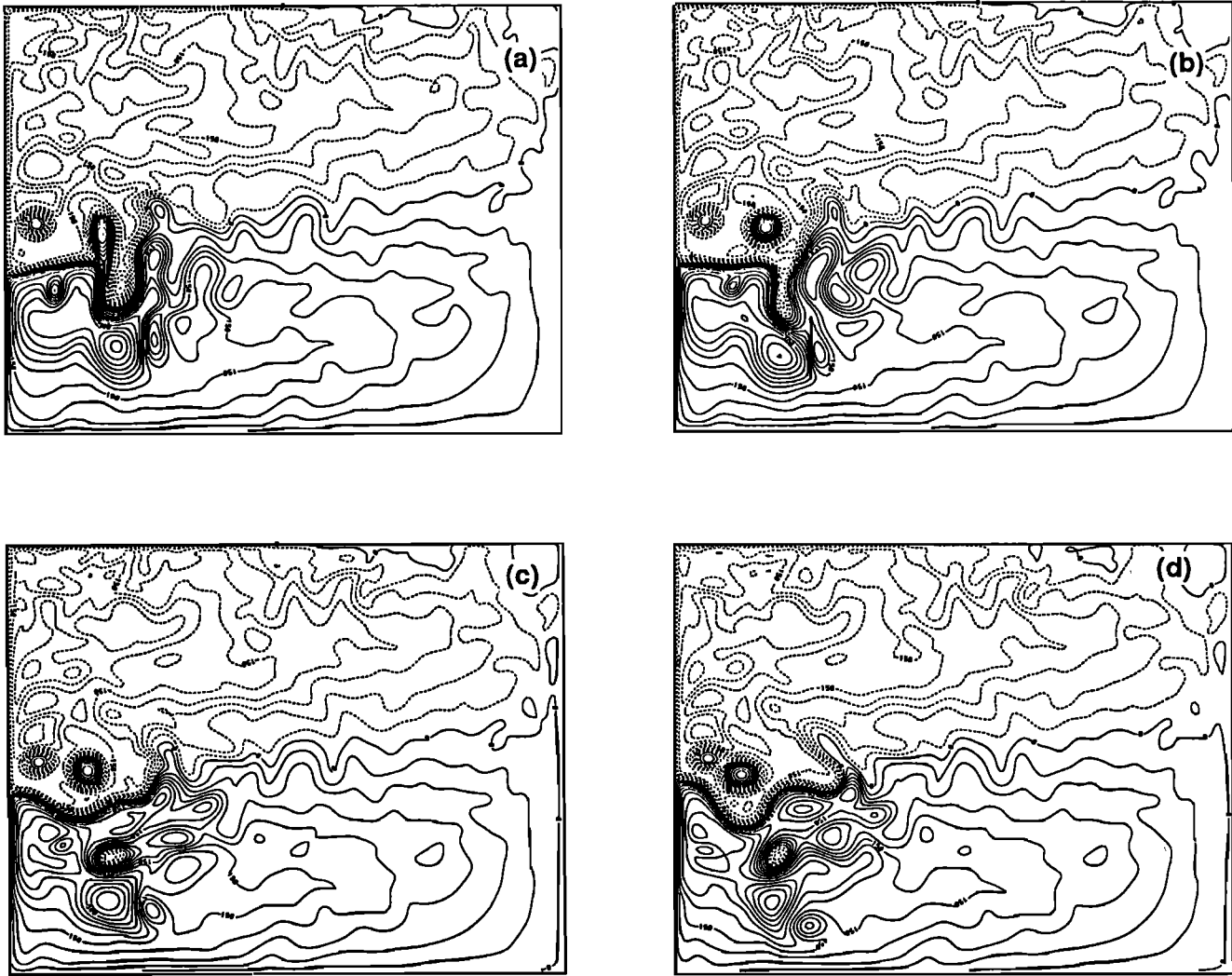


Fig. 4. Typical ring formation event for BB. Each frame represents the interface displacement anomaly in meters (C.I. = 30 m), and the time increment is 10 days.

In SPEM, vigorous meanders occur as in BB (Figure 5), and most of the rings (80 to 90%) form in the first quarter of the domain (Figure 6d). Once formed, they often encounter the mid-latitude jet and are reabsorbed. Fewer rings than in either QG, LBE, or BB reach the western wall. SPEM, like QG, presents a fairly even distribution of the rings loci. The mean position of the mid-latitude jet is only slightly south of the ZWCL (Figure 1d).

#### 4. RING STATISTICS

A summary of the ring statistics is presented in Table 1 and Table 2 for the anticyclones or warm-core rings (WCRs) and for the cyclones or cold-core rings (CCRs), respectively.

##### 4.1. Census

The total number of rings formed during the 10 years after spin-up varies significantly from one numerical model to the other and decreases as more physics are taken into account in the numerical models (109, 87, 76, and 70 rings for QG, LBE, BB, and SPEM, respectively). The statistics for SPEM were performed on a 7-year dataset and extrapolated to a 10-year period. In QG, one would have expected a sym-

metric number of WCRs and CCRs (4.3 and 5.6 per year respectively) because of the symmetric nature of the QG solution. Such was the case in a preliminary study performed by Chassignet and Verron [1989] for a smaller domain ( $2000 \times 2000$  km) where an average of 4 WCRs and 4 CCRs were created per year. One has to keep in mind that the ring count is somewhat subjective. Temporary interactions with the jet may confuse the ring identification by leading to an early termination and initiation of a new ring. The number of WCRs in LBE, BB, and SPEM (4.7, 4, and 4 per year, respectively) is fairly close to QG (4.3 per year). On the other hand, there is a sharp decrease in CCRs from QG (5.6 per year) to LBE (4 per year), BB (3.6 per year), and SPEM (3 per year).

##### 4.2. Lifetimes

The lifetime of a ring varies greatly among the different numerical models as presented in Table 1 and Table 2 and as illustrated by the lifetime frequency histograms for WCRs and CCRs displayed in Figure 7 and 8, respectively. The lifetime of the rings formed in QG is fairly evenly distributed around the average (85 to 95 days). No distinct regimes can

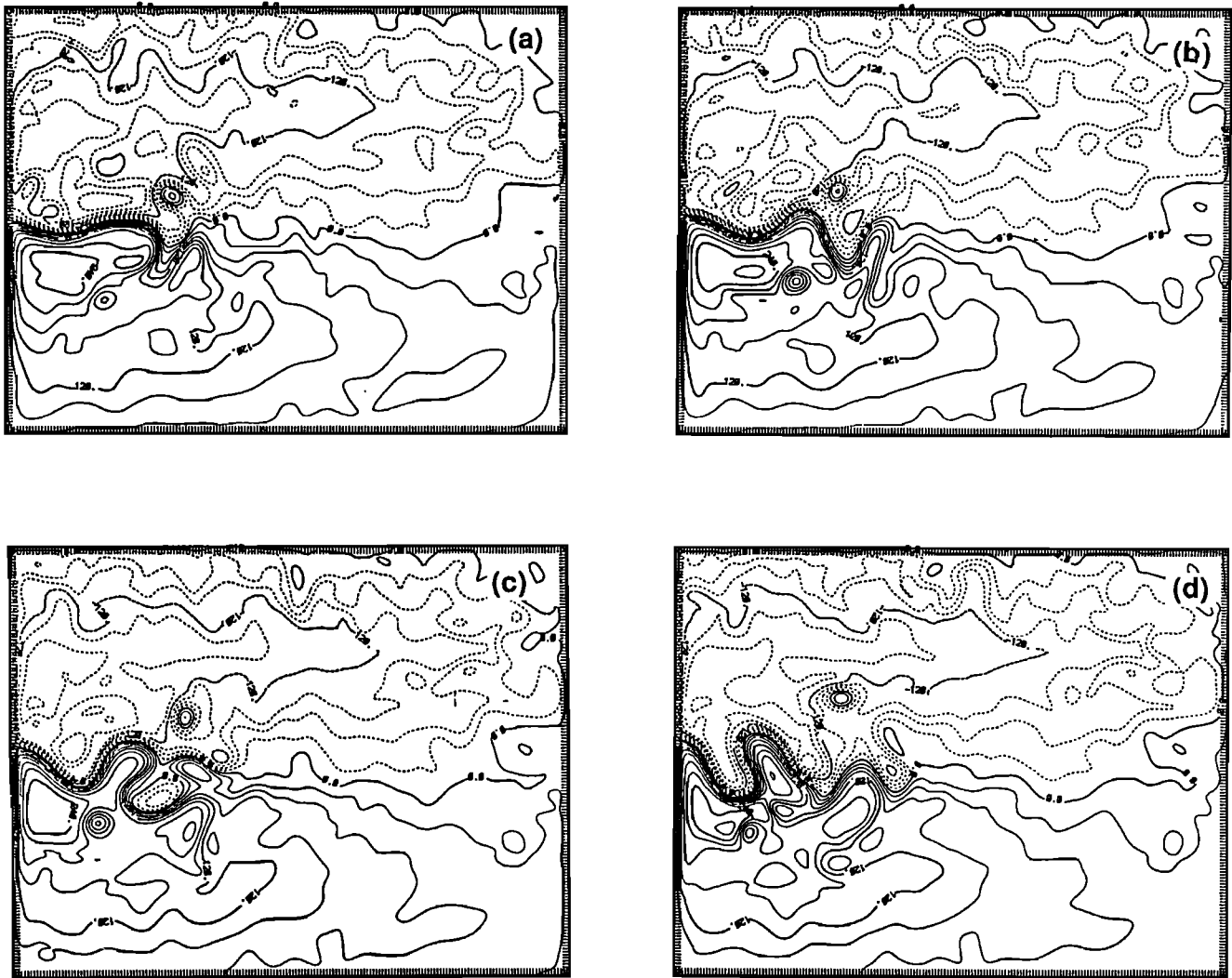


Fig. 5. Typical ring formation event for SPEM. Each frame represents the interface displacement anomaly in meters (C.I. = 30 m), and the time increment is 10 days.

be distinguished. In QG, once a ring is formed (most of the time at the end of the jet as mentioned in the previous section), it propagates westward until it reaches the western wall. Only occasionally does a ring interact with the mid-latitude jet. On the contrary, the ring lifetime in LBE is on the average short (between 40 and 50 days), and the distribution is skewed toward an extremely short lifetime (less than 30 days). This is especially valid for the WCRs (Figure 7b). The LBE mid-latitude jet develops vigorous meanders resulting in rings that are often reabsorbed shortly after formation. In addition, these rings form closer to the western boundary than in QG (Figure 6a and 6b) and therefore have a smaller distance to travel before reaching the western wall and decaying. The latter effect is even more dominant in BB and SPEM, where 70% to 90% of the rings form in the first quarter of the domain (Figure 6c and 6d). In SPEM, the mean lifetime is of the order of 40 days. The ring evolution is different in BB, where on the average, the lifetimes of both WCRs and CCRs are longer (100 and 75 days, respectively). A strong distinction also appears in BB between WCRs and CCRs, since two maxima are present in the WCR distribution (Figure 7c). This is a consequence of the fact

that some WCRs sit and decay very slowly after reaching the western boundary. Once formed, these WCRs have less tendency to interact with the stream when propagating westward because of the southeastern orientation of the stream (Figure 1c). Few or no opportunities are then given to these rings to coalesce with the mid-latitude jet. The maximum lifetime for the WCRs is 200 days versus 150 for QG and LBE and 100 for SPEM. The CCR lifetime distribution in BB is fairly regular (Figure 8c).

It was stated in the preceding paragraph that the ring lifetimes are strongly dependent upon the jet's ability to form vigorous meanders which in turn increase the possibilities for a ring to be reabsorbed. In order to quantify the variability in the jet's location as a function of the models, and thus the chances for a ring to coalesce with the mid-latitude jet, time series of its position at three representative locations (250, 500, and 1000 km east of the western boundary) are displayed in Figure 9 for the four numerical models. As expected, the QG fluctuations are small and are confined to a small band of less than 200 km width around the ZWCL in the three locations (Figure 9a). This does not provide many occasions for a ring to coalesce with the mid-latitude jet. On

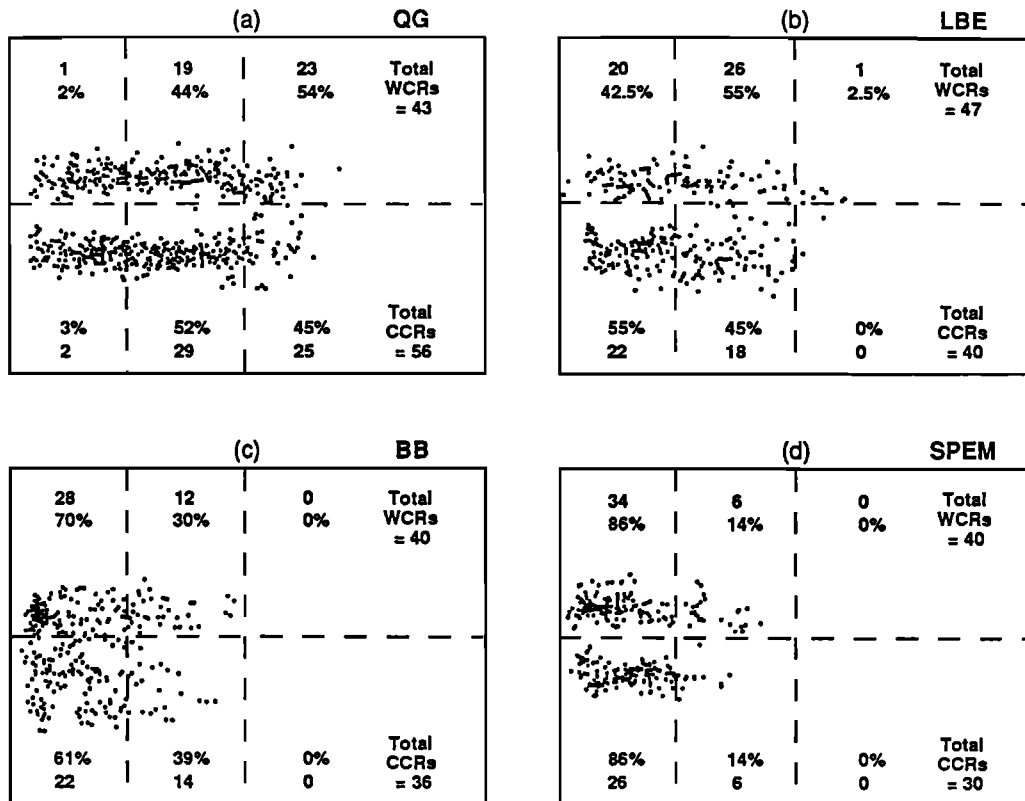


Fig. 6. Ring statistics of the four numerical models (a) QG, (b) LBE, (c) BB, and (d) SPEM: (1) ring location point cloud from the simulations and (2) number of rings formed during a 10-year period in each of the three areas depicted. The spacing in time between two consecutive points is 15 days for QG and LBE and 10 days for BB and SPEM.

TABLE 1. Statistics Over a 10-year Period of the Anticyclonic Rings or Warm Core Rings (WCRs) for (1) the Four Numerical Experiments QG, LBE, BB, and SPEM and (2) the Studies of *Brown et al.* [1986] and *Auer* [1987]

Data Set	Number of WCRs	Average Lifetime, days	Average Radius, km	Interface Displacement, m	Translation Speeds, cm/s	
					Average	RMS
QG	43	84.5	110	120 → 300	15.5	3.1
LBE	47	42	110	120 → 300	14.6	2
BB	40	102	110	120 → 300	9.4	2
SPEM	40	35.9	110	120 → 300	14.5	3.4
<i>Brown et al.</i> [1986]	87	130	75		6.5	1.2
<i>Auer</i> [1987]	220 (140)*					

\* The number in parentheses is for rings whose formation was observed.

the contrary, LBE has greater fluctuations (plus or minus 200 km) in all three locations (Figure 9b), and consequently, the ring lifetimes are shorter. In fact, only 6.5% of the formed WCRs reached the western boundary in LBE versus 35% in QG. More CCRs (27% versus 43% in QG) reached the boundary, but 82% of them interacted with the jet on their way. The jet in BB fluctuates even more (up to 300 km) (Figure 9c) which explains the broader mean in Figure 1c and the frequent interactions of the rings with the jet. Despite these frequent interactions, the ring lifetimes are greater than in SPEM, which also displays a great variability in its jet's position, especially near the western wall (Figure 9d). In

the two most eastward locations (500 and 1000 km east of the western boundary), the variability is not as important. The rings are therefore more likely to be absorbed by the jet when approaching the western boundary (90%). The characteristics of the variability in the jet's position for the four numerical models are summarized in Table 3.

#### 4.3. Translation Speeds, Trajectories, Interface Displacements and Diameters

The translation speeds and corresponding standard deviations for the WCRs and CCRs are presented in Table 1 and

TABLE 2. Statistics Over a 10-year Period of the Cyclonic Rings or Cold Rings (CCRs) for (1) the Four Numerical Experiments QG, LBE, BB, and SPEM and (2) the Studies of Richardson [1983] and Auer [1987]

Data Set	Number of WCRs	Average Lifetime, days	Average Radius, km	Interface Displacement, m	Translation Speeds, cm/s	
					Average	RMS
QG	56	97	100	120 → 300	15.2	2.1
LBE	40	52.5	100	120 → 300	12.2	3.9
BB	36	75.5	110	120 → 300	8.8	1.4
SPEM	30	46.5	110	120 → 300	13.2	2.7
Richardson [1983]					5	
Auer [1987]	280 (130)*					

\* The number in parentheses is for rings whose formation was observed.

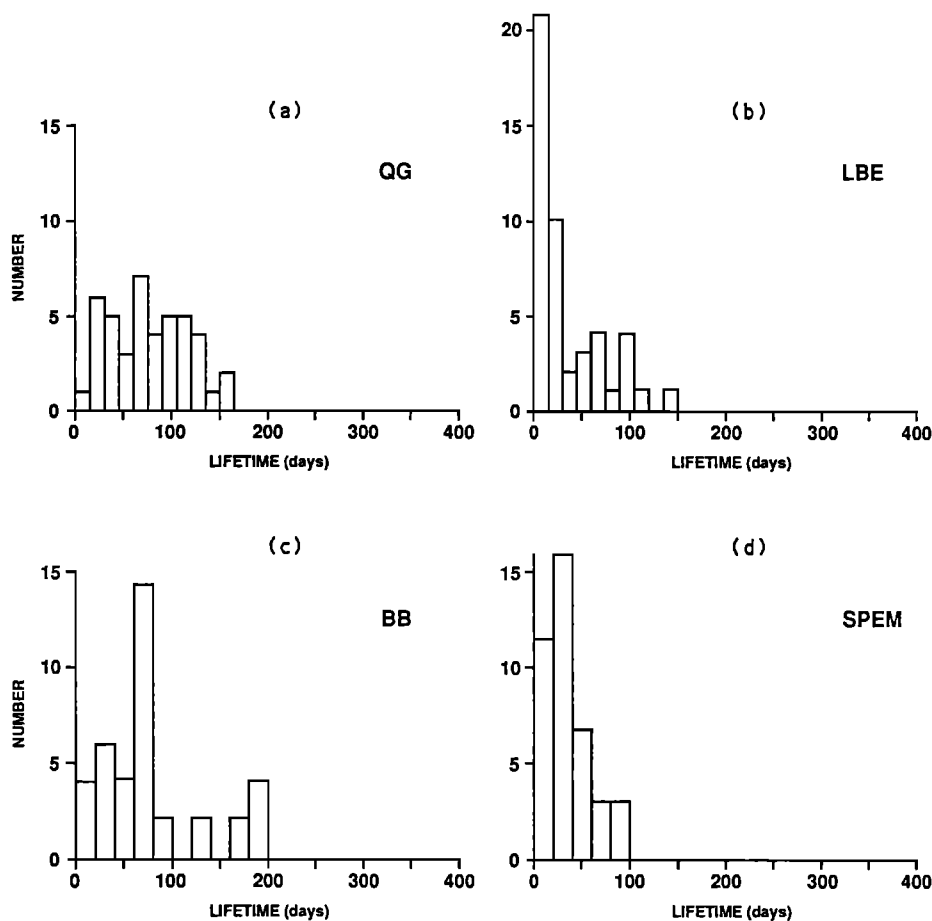


Fig. 7. Lifetime frequency histograms for the WCRs for (a) QG, (b) LBE, (c) BB, and (d) SPEM over a 10-year period.

Table 2, respectively. They were estimated from the long-lived (more than 70 days) rings of each numerical model during time periods when the rings were not strongly interacting with either the mid-latitude jet or the western boundary. A strong interaction is defined in this context as an abrupt change in the direction of propagation (reversal or right angle).

Except for QG, the WCRs propagate significantly faster than the CCRs. This is consistent with the fact that the

westward self-propagation of a cyclone on a  $\beta$  plane is slower than its anticyclonic counterpart [Nof, 1983; Cushman-Roisin et al., 1990]. When the QG approximation is made, this distinction between the westward propagation speeds of anticyclones and cyclones disappears [McWilliams and Flierl, 1979; Cushman-Roisin et al., 1990] and both WCRs and CCRs propagate at the same rate (Table 1 and 2). The translation speeds are overall in agreement between the different numerical models, except for BB where the propagation speed

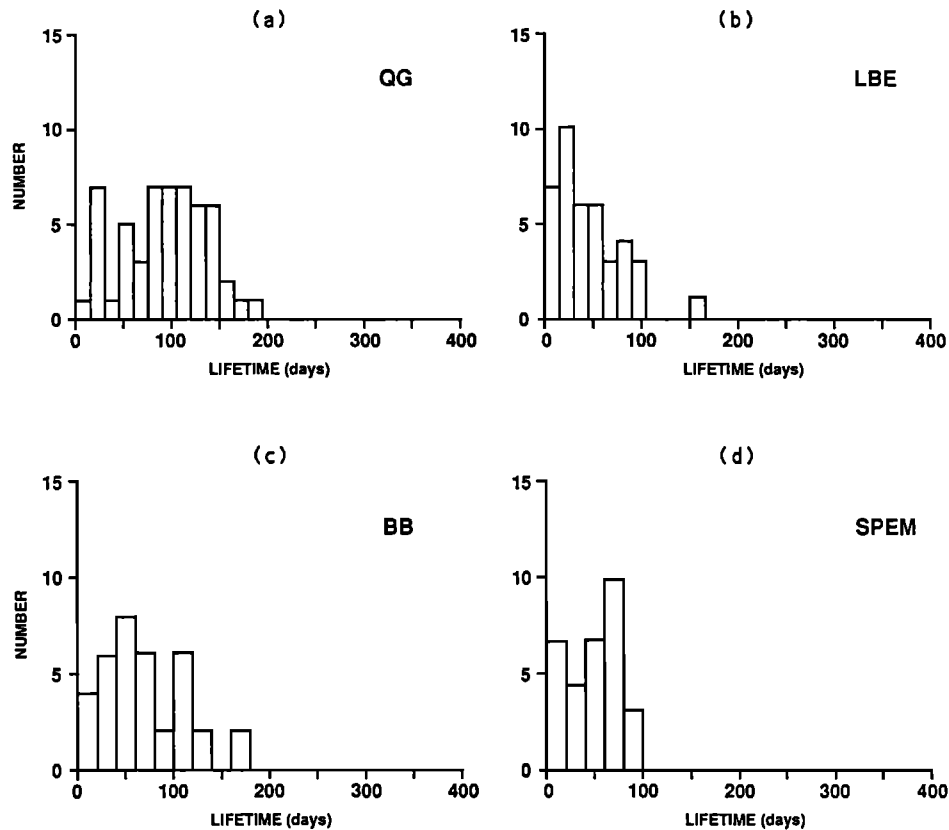


Fig. 8. Lifetime frequency histograms for the CCRs for (a) QG, (b) LBE, (c) BB, and (d) SPEM over a 10-year period.

is slower by about  $5 \text{ cm s}^{-1}$ . The standard deviation varies from 1.4 to 3.9 with the highest being from SPEM and LBE and the lowest from BB (Table 1 and 2). In all models, the rings are observed to slow down as they get close to the mid-latitude jet.

The ring behaviors in each of the numerical models can be further illustrated by the trajectories of five characteristic long-lived rings as displayed in Figure 10. In QG (Figure 10a) the rings propagate westward at a regular pace and only interact occasionally with the mid-latitude jet. In LBE, the trajectories (Figure 10b) are more irregular and interactions are more frequent. In the two primitive equation models BB and SPEM (Figures 10c and 10d), the trajectories are very irregular with strong interactions with the mid-latitude jet and the western wall.

There are no major differences on the average in ring sizes and interface displacements among the models (Tables 1 and 2). The ring radii, defined from the center of the ring to its edge, vary between 80 and 150 km with an average of 100 to 110 km. The corresponding vertical displacement of isopycnals can reach several hundred meters (120 to 300 m). Such displacement is also observed in QG, despite the fact that the QG approximation assumes small displacements for terms to be neglected in the equations.

##### 5. COMPARISON WITH OBSERVATIONS

We are now in a position to discuss the results presented in sections 3 and 4 in relation to observations. Two statistical studies of Gulf Stream rings based on time series of satellite infrared determinations were recently performed over 10-

and 5-year periods, respectively [Brown *et al.*, 1986; Auer, 1987]. The former investigated only Gulf Stream WCRs, since CCRs are difficult to delineate in satellite imagery by surface thermal signal; the CCR sea surface temperature (SST) gradient boundary tends to be weak and the denser cold water core tends to sink with time, wiping out the SST signal. As stated by Auer [1987], an estimate for the CCRs has then to be considered as tentative. In addition, cloudiness can confuse ring identification in infrared images and can lead to an early termination of a ring track and initiation of a new one, therefore overestimating the number of rings formed. However, even if only the rings whose formation is observed are taken into account, Auer's [1987] estimate for the WCRs is higher by a factor of 2 to 3 than that of Brown *et al.* [1986] (Table 1). Since the models' domain is highly idealized (i.e., box domain, no bottom topography), no attempt will be made to judge a model's performance based on a direct comparison, and the observations are then considered only as a reference. In this section the model results are compared with the 10-year statistical analysis of Brown *et al.* [1986].

As more terms are retained in the model governing equations from QG to BB and SPEM, the mid-latitude jet becomes more unstable (Figure 9) and its penetration into the interior is reduced [Holland and Schmitz, 1985]. One would expect an increase in the jet's variability to be correlated with an increase in the number of rings formed, but because of the jet's shorter eastward penetration, this number is actually reduced. This result applies mostly to the CCRs, where a decrease of 40% is observed from QG to BB and SPEM

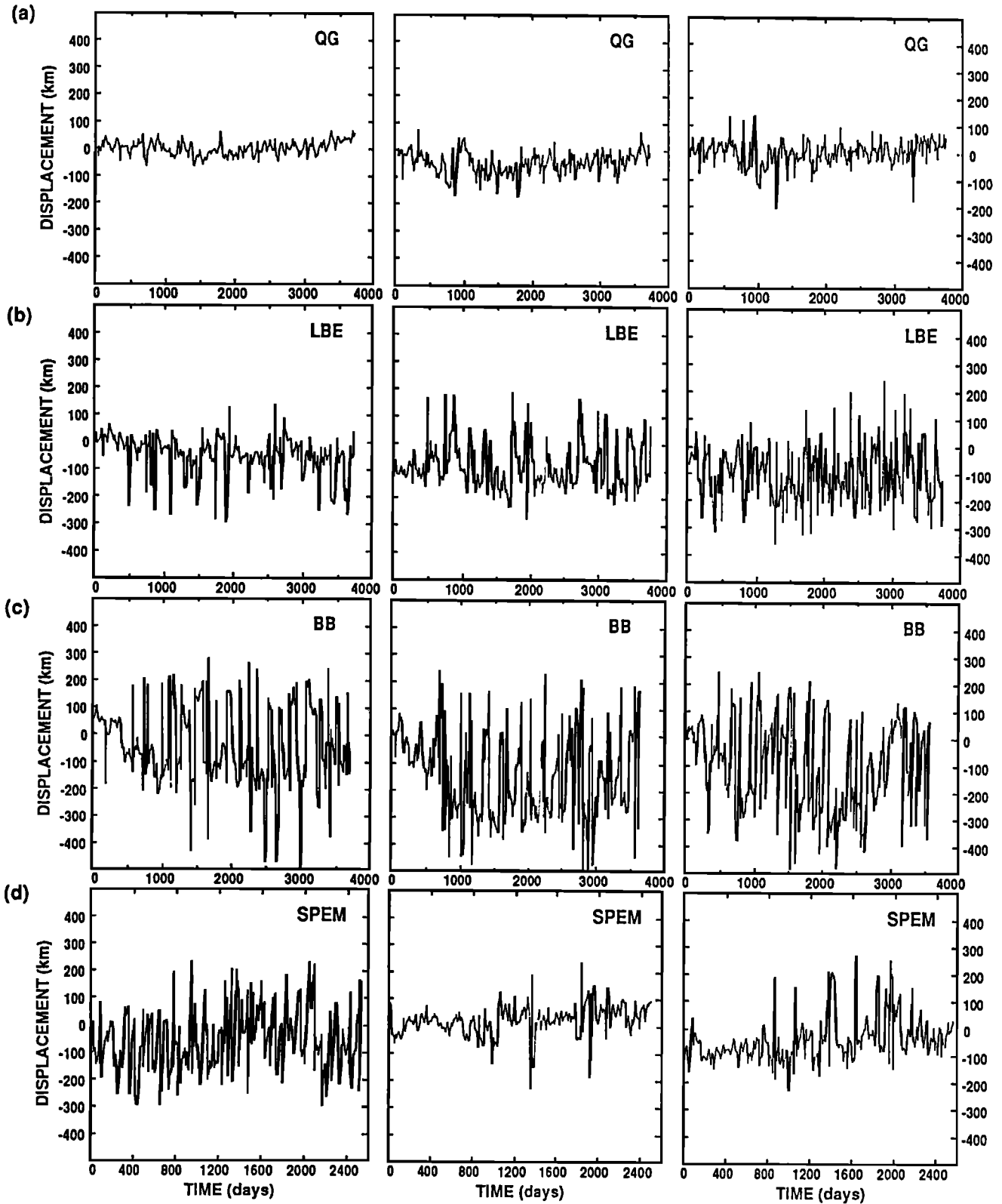


Fig. 9. Time series of the mid-latitude jet position as a deviation from the ZWCL (in kilometers) at three locations (250, 500, and 1000 km east of the western boundary) for the following numerical models: (a) quasi-geostrophic (QG), (b) linear balance (LBE), (c) primitive equation isopycnal coordinates (BB), and (d) primitive equation sigma coordinates (SPEM).

TABLE 3. Characteristics of the Mid-Latitude Jet's Position as a Deviation from the ZWCL in Three Locations A, B, and C for QG, LBE, BB, and SPEM

Numerical Model	Mean Position, km			RMS Displacement, km		
	A	B	C	A	B	C
QG	-1.2	-46.0	-2.0	26.3	42.0	48.7
LBE	-51.4	-79.2	-95.9	75.9	86.9	104.0
BB	-51.3	-142.8	-99.0	150.9	158.1	159.9
SPEM	19.1	-39.2	-51.2	56.8	85.5	114.3

Locations A, B, and C are 250, 500, and 1000 km east of the western boundary, respectively.

(Table 2). The number of WCRs, on the other hand, remains approximately constant among the models (Table 1). In comparison with observations, these numbers are low (Tables 1 and 2). The point location cloud for the 10-year, 87-ring-location time series of *Brown et al.* [1986] is displayed in Figure 11 and is divided into sectors of the same dimensions as Figure 6. A total of 68 rings (78%) were observed to form in the second quarter versus 19 (22%) in the first quarter. This is in agreement with the LBE results (Figure 6b) but not with the two primitive equation models (BB and SPEM), since most of their rings formed in the first quarter of the domain owing to the short jet's eastward penetration. An increase in the jet's penetration scale can be obtained by decreasing the lateral dissipation and by increasing both the vertical and horizontal resolution [*Holland and Schmitz*, 1985; *Barnier et al.*, 1991].

The ring lifetime histogram of *Brown et al.* [1986] is displayed in Figure 12 in a manner similar to Figure 7 for the four numerical models. The distribution is strongly bimodal with means of 55 days for the short-lived rings (less than 140 days) and 230 days for long-lived (more than 140 days). Most of the observed rings which formed in the second quarter (65°-60°W) are short-lived and coalesce with the Gulf Stream around 68°W. The mean lifetime is 130 days and is much greater than in any of the numerical models (Table 1). In QG and LBE, the majority of WCRs form beyond the first quarter of the domain (Figures 6a and 6b) and one would have expected the ring lifetimes to be in agreement with or larger than the observations, at least in QG, since few if any interactions occur between jet and rings and no topographic effects are present in the models. One reason for this discrepancy is that the ring propagation speeds in both QG and LBE are faster than the observed rings by a factor 2 to 3 (Table 1). The rings then reach the western wall in a relatively short period of time. The ring lifetime is even shorter in LBE, since once formed, the rings are almost immediately reabsorbed by the mid-latitude jet. On the other hand, the rings in BB have the longest lifetime of the modeled rings and the smallest average propagation speed (Table 1). It then takes longer for them to reach the western boundary. Furthermore, BB's WCR lifetime distribution is bimodal (Figure 7c), as in the observations, because of long-lived WCRs decaying very slowly after reaching the western wall. This is not the case for the CCRs (Figure 8c). Two explanations can be proposed for this behavior: first, in most cases, the jet has the tendency to separate far south of the ZWCL as in Figure 4, therefore diminishing the

chances for a strong interaction; and second, anticyclonic eddies are in general more robust than their cyclonic counterparts [*Cushman-Roisin and Tang*, 1990]. The latter effect is also valid for LBE and SPEM but does not appear to play a significant role.

Ring translation is caused by a combination of self-induced motion [*Flierl*, 1977; *Nof*, 1983; *Cushman-Roisin et al.*, 1990], advection by the larger scale circulation and interaction with the mid-latitude jet [*Richardson*, 1983; *Olson et al.*, 1985; *Olson and Evans*, 1986; *Cornillon et al.*, 1989; *Chassignet et al.*, 1990]. *Brown et al.* [1986] found the Gulf Stream WCRs to have translation speeds up to 10 times faster than those expected from self-advection. Advection by the larger-scale flows and interaction with the Gulf Stream were then suggested to account for the difference. The model rings also exhibit this more rapid motion. Except for BB, their propagation speeds are in general much faster than in the observations (Tables 1 and 2). Interface displacements are of comparable magnitude [*Olson et al.*, 1985; *Chassignet et al.*, 1990].

## 6. DISCUSSION

The picture resulting from sections 3, 4, and 5 is a ring behavior in BB which differs substantially from that of QG, LBE, or SPEM (slower propagation speed, longer lifetime). The main factor in ring translation speed is the contribution from the background flow, and it is therefore important to determine its strength in the different models. On the one hand, quantification of the intensity of the recirculation gyres is a difficult task, since time averages of the nondivergent upper level/layer stream function (Figure 1) are smoothed by large fluctuations in the jet's position. This is especially valid for BB and SPEM. The velocity distribution indeed varies among the models as a function of the jet penetration length, and one expects substantial differences in the speed of the zonal flows between QG, LBE, and the primitive equation models BB and SPEM. On the other hand, if one considers the ring as a tracer characteristic of the background flow, then QG, LBE, and SPEM have comparable recirculations while that in BB is weaker.

In addition to the large-scale flows, other factors, such as numerical representation of the form stress as the base of the eddy or of the dissipation processes, might be of importance in the ring propagation speed. These factors, presently under investigation in a companion study which focuses on the behavior of rings in a channel first in isolation and then embedded in a mean flow, are discussed in some detail in the remaining of this section.

Let us first consider the ring in isolation (i.e., in the absence of external flows or topography) and with only one active layer. On the  $\beta$  plane, it will propagate westward through self-advection [*Nof*, 1983; *Cushman-Roisin et al.*, 1990] at the speed of a long Rossby wave defined from the undisturbed depth corrected by half the average interfacial displacement over the eddy [*Chassignet and Cushman-Roisin*, 1991]:

$$c = -\frac{\beta g'}{f_0^2} \left( H_1 + \frac{1}{2} \frac{\int \int \eta^2 dx dy}{\int \int \eta dx dy} \right). \quad (2)$$

This expression simplifies when the QG approximation is made, since the contribution due to the interface is neglected. The eddy then propagates at the speed of the long Rossby wave defined from the undisturbed depth only ( $4 \text{ cm s}^{-1}$  for

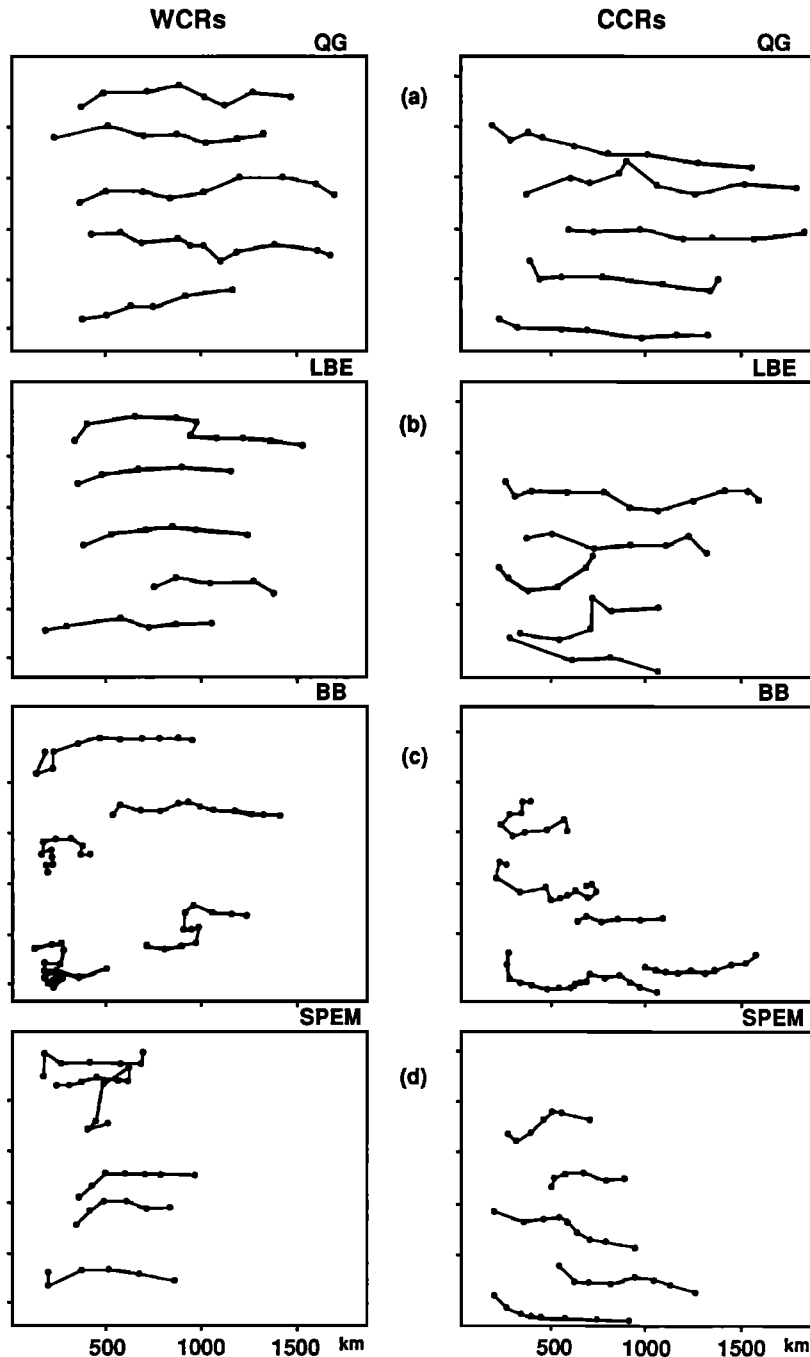


Fig. 10. Trajectories of five characteristic long-lived WCRs and CCRs for the four numerical models (a) QG, (b) LBE, (c) BB, and (d) SPEM. The x axis represents the distance in kilometers from the western boundary while a tick mark on the y axis represents the position of the ZWCL for each ring. The time period between two dots is 15 days for QG and LBE and 10 days for BB and SPEM.

the stratification used in the models). Variations in propagation speed due to the model formulation or due to ring size, shape, or volume are at most of the order of the correction induced by the averaged displacement of the interface [Cushman-Roisin et al., 1990] and not sufficient to account for the observed differences in propagation speed. The main effect is to slow down cyclones and accelerate anticyclones as is illustrated in section 4.3.

In a finite-depth fluid, the derivation for the westward propagation leads to additional terms [Cushman-Roisin et al., 1990]. The derivation of the westward drift speed of

an isolated eddy in a two-layer system is not repeated here and is given by Cushman-Roisin et al. [1990]. In terms of dimensional variables, the westward propagation speed of the center of mass  $c$  is expressed as

$$c = -\frac{\beta g'}{f^2} \frac{H_2}{H_1 + H_2} \frac{\int \int (H_1 \eta + \frac{1}{2} \eta^2) dx dy}{\int \int \eta dx dy} - \frac{1}{\rho_0 f_0} \frac{\int \int \eta \pi_y dx dy}{\int \int \eta dx dy} \quad (3)$$

where  $H_i$  are the layer thicknesses,  $\eta$  is the interface displace-

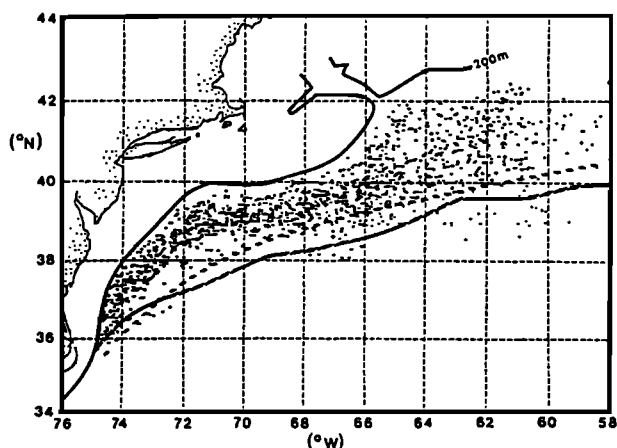


Fig. 11. Point location cloud for the 10-year, 87-ring-location time series of Brown *et al.* [1986]. The dashed line (solid-dashed) represents the Gulf Stream north wall location derived from climatological (satellite-derived) data.

ment, and  $\pi$  is the bottom-layer pressure. The first term is the equivalent to the expression for the one-layer system multiplied by the factor  $H_2/(H_1 + H_2)$ , while the second term is a twisting term acting as a form stress on the eddy. This result was derived for a two-layer system but still holds for several moving layers if the pressure field  $\pi$  is defined in the second layer below the surface. In a physical sense, an anticyclone can be viewed as an obstacle which, as it moves, forces the surrounding fluid to part. On the other hand, a cyclone forces the surrounding fluid to converge.

If the ring is embedded in a mean flow, then the effect of baroclinicity on the ring propagation speed will be a function of the initial potential vorticity distribution in the lower layers and, as is shown by studies such as those of McWilliams and Flierl [1979], Mied and Lindemann [1979], and Smith and Ried [1982], different initializations yield different or opposite behaviors. The form stress is likely to become important as the surrounding fluid in the lower layer is forced to part faster as the ring is entrained, therefore generating resistance to the ring motion. Previous studies on the contribution of a mean flow concentrated mostly on the motion of the eddy relative to this mean flow [Holland, 1983; Cornillon *et al.*, 1989] by making use of simple barotropic or equivalent-barotropic models. In their study of the influence of the slope water on warm-core ring propagation, Cornillon *et al.* [1989] ignored the form stress at the base of the eddy by assuming the lower layer to be at rest, therefore neglecting the term involving  $\pi_y$ . As they stated, it is also equivalent to assuming that the flow in the lower layer has a sufficient north-south symmetry such that the form stress vanishes. Such a situation is unlikely to occur in reality, and it is reasonable to expect the form stress to oppose the ring's westward propagation as the surrounding water is forced to part. The question then arises as to what extent the representation of this form stress differs from one model to the other.

A slow propagation speed is related to a long ring lifetime, but other factors such as resolution of the ring fronts or representation of the lateral dissipation will also affect the ring structure evolution and lifetime. Because of a higher resolution of gradients and lack of cross-isopycnal numerical

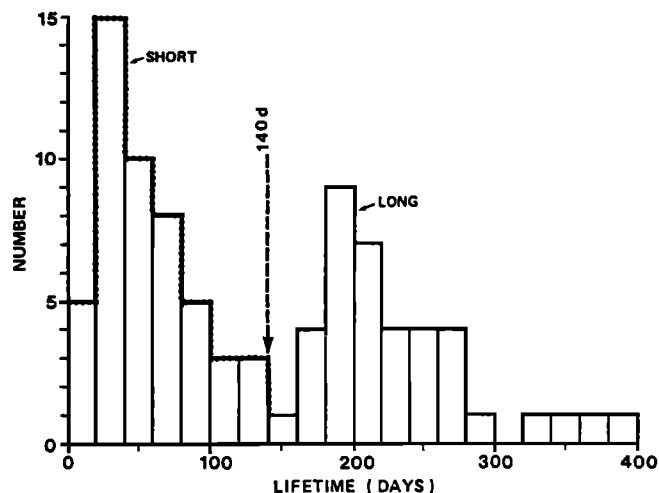


Fig. 12. Ring lifetime histogram over a 10-year period after Brown *et al.* [1986]. Short lived rings (less than 140 days) are outlined by dots. Mean ring age is 130 days.

diffusion, one might expect that a ring in the layer coordinate system will conserve its shape longer (i.e., less diffusion and slower decay) than an equivalent ring in a level coordinate system. A more robust ring also means a better chance of survival to an eventual interaction with the mid-latitude jet. This is in agreement with the fact that rings in BB are observed to conserve their strength (characterized by their maximum interface displacement) even after strong interactions with the jet or the western boundary current. In the other numerical models, on the contrary, a significant decay in the ring strength is observed after each interaction. When in isolation, the ring retains its identity, and no significant differences in decay are observed between the models. Independently of the fact that the rings in BB propagate more slowly, one expects them to possess a longer lifetime because of their robustness. A more robust structure might also emphasize the tendency for anticyclones to be more stable than cyclones.

## 7. SUMMARY AND CONCLUDING REMARKS

Significant differences are observed in ring formation and behavior among numerical models with different physical assumptions or numerics. Ring locus, lifetime, propagation speed, radius, and interface displacement statistics were derived for four widely used eddy-resolving numerical models and compared with the 10-year statistical analysis of Gulf Stream rings based on time series of satellite infrared determinations performed by Brown *et al.* [1986]. It was shown that as more terms are retained in the model governing equations, the mid-latitude jet becomes more unstable and its interior penetration length scale is reduced. Despite an increase in the jet's variability, the number of rings decreases as well because of the shorter jet's penetration. In addition, rings in the layer model have slower propagation speeds and longer lifetimes than their level counterparts. Factors which may be responsible for the differences are the strength of the recirculation gyres, the importance of the form stress at the base of the eddy, and the numerical representation of the dissipation processes. This study then provides a starting point from which these specific aspects can be investigated in a less complex setting.

Because of the importance of rings in the ocean energetics and general circulation [Olson, 1991], a proper representation of their formation and behavior in numerical models is crucial if one wants an accurate picture of the heat, salt, and energy budgets. The results presented in this paper illustrate the sensitivity of numerical ocean circulation models to the physical and numerical assumptions made.

*Acknowledgments.* The author would like to thank J. Verron for initiating this study. P. Gent and D. Haidvogel gave valuable assistance with interpretation of the results. Conversations with B. Cushman-Roisin and C. Rooth were timely and valuable. Many thanks to D. Haidvogel for providing the SPEM data sets. N. Norton built the QG and LBE models used in this study and helped analyze the results. The computations were carried out using the CRAYS at the National Center for Atmospheric Research (NCAR). NCAR is sponsored by the National Science Foundation.

## REFERENCES

- Auer, S. J., Five-year climatological survey of the Gulf Stream system and its associated rings, *J. Geophys. Res.*, **92**, 11,709-11,726, 1987.
- Barnier, B., B. L. Hua and C. Le Provost, On the catalytic role of high baroclinic modes in eddy-driven large-scale circulation, *J. Phys. Oceanogr.*, **21**, 976-997, 1991.
- Bleck, R., and D. B. Boudra, Initial testing of a numerical ocean circulation model using a hybrid (quasi-isopycnic) vertical coordinate, *J. Phys. Oceanogr.*, **11**, 755-770, 1981.
- Bleck, R., and D. B. Boudra, Wind-driven spin up in eddy-resolving ocean models formulated in isopycnic and isobaric coordinates, *J. Geophys. Res.*, **91**, 7611-7621, 1986.
- Bryan, F. O., and W. R. Holland, A high resolution simulation of the wind- and thermohaline-driven circulation in the North Atlantic Ocean, in Proceedings, 'Aha Huliko'a Hawaiian Winter Workshop, edited by P. Muller and D. Anderson, pp. 99-115, University of Hawaii, Honolulu, 1989.
- Bryan, K., A numerical model for the study of the world ocean, *J. Comput. Phys.*, **4**, 347-376, 1969.
- Brown, O. B., P. C. Cornillon, S. R. Emmerson, and H. M. Carle, Gulf Stream warm rings: A statistical study of their behavior, *Deep Sea Res.*, **33**, 1459-1473, 1986.
- Chassignet, E. P., and D. B. Boudra, Dynamics of Agulhas retroreflection and ring formation in a numerical model, II, Energetics and ring formation, *J. Phys. Oceanogr.*, **18**, 304-319, 1988.
- Chassignet, E. P., and B. Cushman-Roisin, On the influence of a lower layer on the propagation of nonlinear oceanic eddies, *J. Phys. Oceanogr.*, **21**, 939-957, 1991.
- Chassignet, E. P., and P. R. Gent, The influence of boundary conditions on mid-latitude jet separation, *J. Phys. Oceanogr.*, **21**, 1290-1299, 1991.
- Chassignet, E. P., and J. Verron, Rings in numerical models of ocean general circulation, in *Proceedings of the 7th Symposium on Turbulent Shear Flows*, pp. 18.2.1-18.2.6, Stanford University, Stanford, Calif., 1989.
- Chassignet E.P., D.B. Olson, and D.B. Boudra, Motion and evolution of oceanic rings in a numerical model and in observations, *J. Geophys. Res.*, **95**, 22,121-22,140, 1990.
- Cornillon, P., R. Weyer, and G. Flierl, Translational velocity of warm core rings relative to the slope water, *J. Phys. Oceanogr.*, **19**, 1317-1332, 1989.
- Cox, M., A primitive equation three-dimensional model of the ocean, *Tech. Rep.*, **1**, NOAA Geophys. Fluid Dyn. Lab., Princeton Univ., Princeton, N. J., 1984.
- Cushman-Roisin, B., and B. Tang, Geostrophic turbulence and emergence of eddies beyond the radius of deformation, *J. Phys. Oceanogr.*, **20**, 97-113, 1990.
- Cushman-Roisin, B., E.P. Chassignet, and B. Tang, Westward motion of mesoscale eddies, *J. Phys. Oceanogr.*, **20**, 758-768, 1990.
- Flierl, G.R., The application of linear quasigeostrophic dynamics to Gulf Stream rings, *J. Phys. Oceanogr.*, **7**, 365-379, 1977.
- Gent, P. R., and J. C. McWilliams, Regimes of validity for balanced models, *Dyn. Atmos. Oceans*, **7**, 167-183, 1983.
- Haidvogel, D. B., J. L. Wilkin, and R. Young, A semi-spectral primitive equation ocean circulation model using vertical sigma and orthogonal curvilinear horizontal coordinates, *J. Comput. Phys.*, **94**, 151-185, 1991.
- Holland, G. J., Tropical cyclone motion: Environmental interaction plus a beta effect, *J. Atmos. Sci.*, **40**, 328-342, 1983.
- Holland, W. R., The role of mesoscale eddies in the general circulation of the ocean - Numerical experiments using a wind-driven quasi-geostrophic model, *J. Phys. Oceanogr.*, **8**, 363-392, 1978.
- Holland, W. R., and L. B. Lin, On the generation of mesoscale eddies and their contribution to the oceanic general circulation, I, A preliminary numerical experiment, *J. Phys. Oceanogr.*, **5**, 642-657, 1975.
- Holland, W. R., and W. J. Schmitz, Zonal penetration scale of model mid-latitude jets, *J. Phys. Oceanogr.*, **15**, 1859-1875, 1985.
- Hurlburt, H. E., and J. D. Thompson, A numerical study of Loop Current intrusions and eddy shedding, *J. Phys. Oceanogr.*, **10**, 1611-1651, 1980.
- Ikedo, M., Meanders and detached eddies of a strong eastward-flowing oceanic jet using a two-layer quasi-geostrophic model, *J. Phys. Oceanogr.*, **11**, 526-540, 1981.
- Lorenz, E. N., Energy and numerical weather prediction, *Tellus*, **12**, 364-373, 1960.
- McWilliams, J.C., and G.R. Flierl, On the evolution of isolated non-linear vortices, with application to Gulf Stream rings, *J. Phys. Oceanogr.*, **9**, 1155-1182, 1979.
- McWilliams, J. C., N. J. Norton, P. R. Gent, and D. B. Haidvogel, A linear balance model of wind-driven, mid-latitude ocean circulation, *J. Phys. Oceanogr.*, **20**, 1349-1378, 1990.
- Mied, R.P., and G.J. Lindemann, The propagation and evolution of cyclonic Gulf Stream rings, *J. Phys. Oceanogr.*, **9**, 1183-1206, 1979.
- Nof, D., On the migration of isolated eddies with application to Gulf Stream rings, *J. Mar. Res.*, **41**, 399-425, 1983.
- Olson, D. B., Rings in the ocean, *Annu. Rev. Earth Planet. Sci.*, **19**, 283-311, 1991.
- Olson, D.B., and R.H. Evans, Rings of the Agulhas, *Deep-Sea Res.*, **33**, 27-42, 1986.
- Olson, D.B., R.W. Schmitt, M. Kennelly, and T.M. Joyce, A two-layer diagnostic model of the long-term physical evolution of warm-core ring 82B, *J. Geophys. Res.*, **90**, 8813-8822, 1985.
- Pedlosky, J., *Geophysical Fluid Dynamics*, 624 pp., Springer-Verlag, New York, 1979.
- Richardson, P. L., Gulf Stream rings, in *Eddies in Marine Science*, edited by A. R. Robinson, pp. 19-45, Springer-Verlag, New York, 1983.
- Semtner, A. J., and R. M. Chervin, A simulation of the global ocean circulation with resolved eddies, *J. Geophys. Res.*, **93**, 15,502-15,522, 1988.
- Smith, D. C., IV, and R. O. Reid, A numerical study of non-frictional decay of mesoscale eddies, *J. Phys. Oceanogr.*, **12**, 244-255, 1982.
- Spall, M. A., and A. R. Robinson, Regional primitive equation studies of the Gulf Stream meander and ring formation region, *J. Phys. Oceanogr.*, **20**, 985-1016, 1990.
- Verron, J., and C. Le Provost, Response of eddy-resolved general circulation numerical models to asymmetrical wind forcing, *Dyn. Atmos. Oceans*, in press, 1992.

E. Chassignet, RSMAS/MPO, University of Miami, 4600 Rickenbacker Causeway, Miami, FL 33149.

(Received October 18, 1991;  
revised February 7, 1992;  
accepted April 6, 1992.)